Journal of Magnetism and Magnetic Materials 491 (2019) 165621

Contents lists available at ScienceDirect

Journal of Magnetism and Magnetic Materials

journal homepage: www.elsevier.com/locate/jmmm

Research articles

Magnetic permeability measurement for steel pipe immersed in geomagnetic field

Huang Xinjing[a,c], Liu Shan[a,b,c,*], Zeng Zhoumo[a,c], Li Jian[a,c]

[a] State Key Laboratory of Precision Measuring Technology and Instruments, Tianjin University, Tianjin, China
[b] North China Institute of Aerospace Engineering, Langfang 065000, China
[c] Binhai International Advanced Structural Integrity Research Centre, Tianjin 300072, China

ARTICLE INFO

Keywords:
Pipeline
Magnetic field
Permeability measurement

ABSTRACT

This paper demonstrates a method of measuring the permeability of a pipe based on the magnetic shielding effect via simulations and experiments. Short pipe specimens are directly cut from a long industrial pipe instead of machining the pipe into strip, rod, or ring specimens. During measurement, the pipe specimen immersed in the geomagnetic fields rotates around a vertical axis and the magnetic fields inside are simultaneously recorded. It is found that original magnetizations can induce magnetic bias inside the pipe, which can be calculated and removed by using the recorded fields as a function of rotation angle. The magnetic fields without bias are used to calculate the shielding factor and then uniquely determine the pipe permeability based on the pipe shielding model. Since employing a pipe itself as the specimen can avoid additional magnetization generated during re-manufacturing, the measured permeabilities by the proposed method can be used as permeability samples and references for an on-site pipeline during magnetic abnormity inspections.

1. Introduction

Steel pipelines are the most important infrastructure for transporting oil and natural gas. Security issues are one important aspect of pipeline operation management. Magnetic measurement of pipeline deformation and displacement is a novel and promising inspection method for pipeline integrity [1,2]. Magnetic permeability is a key parameter for magnetic inspections of a pipeline.

First, the magnetic shielding factor of the pipeline depends on the magnetic permeability, in addition to the pipe diameter and wall thickness [3–5]. Therefore, the permeability accuracy employed determines the calculation accuracy of the pipeline direction and trajectory by using the magnetic fields inside the pipeline based on the magnetic shielding effects [6,7]. Second, when the pipeline is displaced due to the scouring of ocean currents or the movement of the seabed, the stress of the pipeline accordingly changes [8,9]. Then the pipeline permeability also changes due to the magneto-mechanical effects [10], which can cause the change of the magnetic fields inside the pipeline. Therefore, via beforehand measuring the magnetic permeability of a pipeline with no stress change, the pipeline shielding factor and the internal magnetic fields under normal conditions can be calculated as important contrasts to those when abnormal deformation and displacement changes occur.

There are many methods for determining the magnetic permeability of a ferromagnetic material sample, but few suitable for a pipeline. Most commonly, a coil is wound around a cylindrical or toroidal sample and a low frequency alternating current is applied to the coil [11], and the permeability is thus found from the impedance of the coil. Or according to the definition, two coils are used, one to measure the magnetic flux density in the sample and the other one to generate excitation magnetic fields with a known intensity, and then the ratio of the two fields is the permeability [12,13]. For the plate specimen, the permeability can be determined by calculating the ratio of the mutual inductance values with and without the specimen situated in the gaps formed by a pair of cores [14]. This method is suitable for large plate specimens so that the tedious preparation of specimens with special shapes is unnecessary.

As magneto-mechanical effects are ubiquitous for pressurized vessels and pipes, apparatuses for revealing the effects of stress on the magnetic permeability has also been developed. Makar proposed an apparatus that can simultaneously stress and magnetize a steel rod for in-situ measurement of the differential permeability under stress [15,16]. The apparatus consisted of a strain gauge that was used to measure the strain on the sample, a coil that was used to measure the flux density experienced by the sample, and a Hall probe that was used to measure the magnetic field applied to the sample. Langman proposed

* Corresponding author at: North China Institute of Aerospace Engineering, Langfang 065000, China.
E-mail address: lshan1006@tju.edu.cn (L. Shan).

https://doi.org/10.1016/j.jmmm.2019.165621
Received 26 March 2019; Received in revised form 17 July 2019; Accepted 20 July 2019
Available online 22 July 2019
0304-8853/

a new method of measuring the permeability of biaxially stressed steel plate with vertically magnetization based on the magnetomotive-force–vane method [17]. C-shaped yoke iron was employed to vertically magnetize the steel plate at very low frequency (1–2 Hz) and the in-plane force is applied to the plate along the two horizontal axes.

When applying these methods above to pipes, the pipe must be manufactured into rod, ring, and plate specimens and large residual stress is inevitably introduced. Due to the magneto-mechanical effects, the permeability of the specimen is completely different from that of the in-situ pipeline.

Eddy current (EC) testing is a possible method of in-situ measuring the AC permeability of a pipe via local electromagnetic excitations. Yu found the conductivity invariance (CI) phenomenon and used CI to separate the impacts of the electrical conductivity and the magnetic permeability of the sample making permeability measurement possible [18]. Lu proposed a compensation scheme with regards to the phenomenon of the decrease in zero-crossing frequency with the increase of liftoff. Such compensation can reduce the errors due to liftoff variances in estimating both the permeability and zero-crossing frequency via multi-frequency eddy current measurements [19]. Han proposed a method of rapidly measuring the magnetic permeability and losses of structural steel immersed in weak sinusoidal magnetic fields based on dynamic magnetization with the frequency of 50–300 Hz [20]. Ideally, the EC probe can be manufactured into a small enough size to fit well the curved pipe wall and implement the in-situ measurement of the pipe permeability, but can only measure the AC and local permeability that is not equal to the permeability of the pipeline sections immersed in weak and DC geomagnetic fields.

Instead, Desjardins and Luo via deploying the coils coaxial with the pipe used EC method to measure the overall permeability of a small pipe [21,22]. In [21], the excitation and pick-up coils were outside the pipe, while in [22], the coils were inside the pipe. This method is based on the dependence of the propagation impedance between the transmitting and receiving coils on the permeability. However, this method is impractical for a field pipeline, as the diameter is too large for the coil to generate large enough electromagnetic fields covering the pipe section.

This paper proposes a method for measuring the overall DC permeability of a steel pipe immersed in geomagnetic field based on the magnetic shielding effect. Instead of machining the pipe into strip, rod, or ring specimens, the tested specimen is a section of an intact pipe that has already gone through all the manufacture procedures. The test only needs to rotate the pipe around the vertical axis in an open area, and measure the internal magnetic fields to calculate the permeability. The pipe permeability measured by this method is equal to that of a field pipeline and are therefore of great significance for the magnetic inspections of on-site pipelines. This paper will demonstrate the validity of the proposed method via simulations and experiments.

2. Measurement principle

Ferromagnetic cavity attenuates the ambient magnetic fields that enter the cavity, which is known as the magnetic shielding effect and is measured by the magnetic shielding factor in a certain direction:

$$\lambda = B_{in}/B_{out} \tag{1}$$

wherein, B_{in} is the flux density in the cavity and B_{out} is the flux density outside the cavity.

Classical magnetic shielding model formulates the radial magnetic shielding factor λ_r of a cylindrical shell, namely a pipe, as follows [5]:

$$\lambda_{\text{r}} = \frac{4p}{\mu_r(p-1)+2(p+1)} \tag{2}$$

wherein $p = \frac{(b+t)^2}{b^2}$, b is the inner radius, t is the wall thickness, and μ_r is the magnetic permeability (Fig. 1). After the magnetic shielding factor

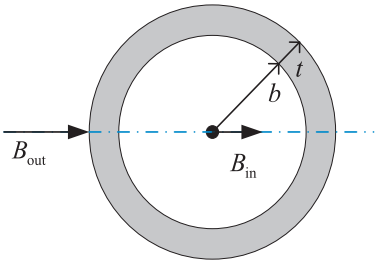

Fig. 1. Cylindrical magnetic shield cavity.

is calculated by using the measured internal and external magnetic fields, the magnetic permeability can be calculated as:

$$\mu_r = \frac{4p}{\lambda_r(p-1)} - 2\frac{p+1}{p-1} \tag{3}$$

However, the original magnetization in the pipe wall will introduce fixed original magnetic fields inside the pipe, which need to be removed before calculating the shielding factor and permeability.

Establish the global earth coordinate system O-$X_eY_eZ_e$ and the pipe coordinate system O-$X_pY_pZ_p$ as shown in Fig. 2. The axes X_e, Y_e, Z_e point to the east, north and the sky, respectively. The axis X_p is parallel to the pipe axis, Y_p is horizontal and perpendicular to the pipe axis, and Z_p is parallel to Z_e. The pipe is rotated together with O-$X_pY_pZ_p$ around the axis Z_p. The rotation angle is denoted as φ, $\varphi \in [0^\circ, 360^\circ]$. In two cases with and without the steel pipe, the magnetic field at the center of the pipe measured by the magnetometer can be expressed as:

$$B_{mY} = \lambda_r B_0 \cos\theta_0 \cos(\varphi + \varphi_0) + \bar{B_Y} \tag{4}$$

and

$$B'_{mY} = B_0 \cos\theta_0 \cos(\varphi + \varphi_0) \tag{5}$$

where θ_0, φ_0, B_0 are the magnetic inclination, declination and norm of the geomagnetic field, and $\bar{B_Y}$ is the magnetic bias caused by original magnetizations. $\bar{B_Y}$ can be determined by using the maximum and minimum of B_{my} as follows:

$$\bar{B_Y} = (B_{mY\max} + B_{mY\min})/2 \tag{6}$$

The magnetic shielding factor is calculated as Eq. (7) and then substituted into Eq. (3) to calculate the permeability. Both the y and z axes are along the radial direction of the pipe. Since the pipe is axisymmetric, the results of calculating the radial shielding factor using these two components are the same. This paper only uses y component to measure the axial shielding factor to calculate the permeability.

$$\lambda_r = (B_{mY} - \bar{B_Y})/B'_{mY} \tag{7}$$

3. Simulation verifications

3.1. Magnetic shielding factors of homogeneous pipes

The radial magnetic shielding factors of pipes with different wall thicknesses and diameters are calculated via two methods: finite

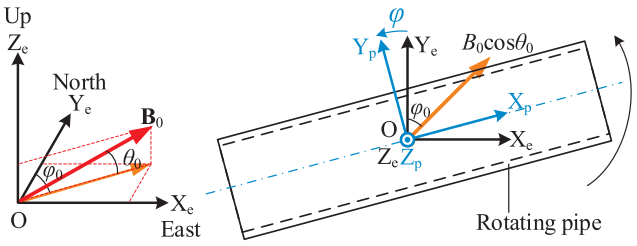

Fig. 2. Definition of the rotating pipe coordinate system.

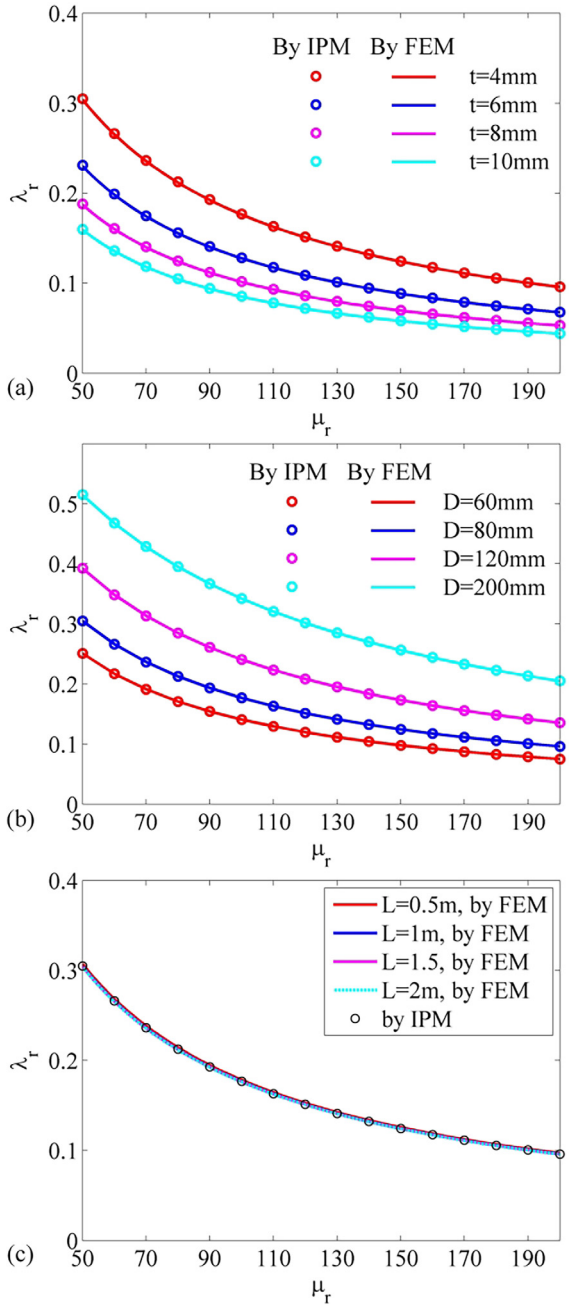

Fig. 3. Radial magnetic shielding factors of pipes with different *t*, *D* and *L*.

element simulation and infinite pipe model (IPM). The finite element simulation is implemented by COMSOL software. The steel pipe is placed in air domain and ambient fields are provided as follows:

$$H_x = H_0\cos\theta_0 \sin\varphi_0$$
$$H_y = H_0\cos\theta_0\cos\varphi_0$$
$$H_z = -H_0\sin\theta_0 \quad (8)$$

where $H_0 = B_0/\mu_0$. In Tianjin, $\theta_0 = 58.7^\circ$, $\varphi_0 = 5.8^\circ$, and $H_0 = 40$ A/m.

The sweeping range of the relative magnetic permeability of the pipe is set as $\mu_r \in [50,200]$. Three groups of simulations are performed: (1) Pipe length $L = 2$ m, diameter $D = 80$ mm, wall thickness $t \in \{4$ mm, 6 mm, 8 mm, 10 mm$\}$; (2) Pipe length $L = 2$ m, wall thickness $t = 4$ mm, diameter $D \in \{60$ mm, 80 mm, 120 mm, 200 mm$\}$; (3) pipe diameter $D = 80$ mm, wall thickness $t = 4$ mm, length $L \in \{0.5$ m, 1 m, 1.5 m, 2 m$\}$. The results of two methods are shown in Fig. 3. For pipes with different wall thicknesses, diameters and lengths, λ_r decreases with the increase of μ_r. Two methods confirm each other's correctness when calculating λ_r. The change of pipe length has no effect on λ_r, which indicates that the pipe sample adopted in experiments does not have to be very long.

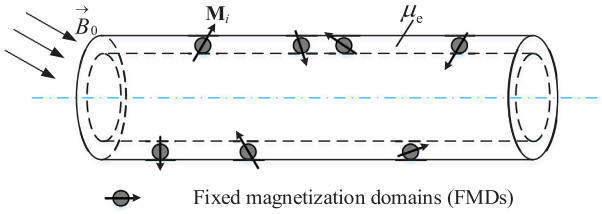

Fig. 4. A pipe containing randomly distributed original magnetizations.

3.2. Magnetic shielding factors of pipes containing original magnetizations

Considering the pipeline may contain original magnetizations, in the simulation model fixed magnetization domains (FMDs) are randomly distributed in the pipe wall, and the magnitude and direction of the magnetization $\mathbf{M}_i$ (i = 1, 2…) of each FMD are also random, as shown in Fig. 4. The magnetic permeability of the remaining portion excluding the FMDs is μ_e. Totally, five groups of simulations are performed: pipes containing 1, 2, 3, 10 and no FMDs. For each group of simulation, φ_0 is swept in the range of $\varphi_0 \in [0^\circ, 360^\circ]$, which is equivalent to the scenario that the pipe is rotated around the vertical axis in a fixed geomagnetic field. The midpoint on the pipe axis is selected as the observation point.

The results of B_y-φ curve simulations are shown in Fig. 5. For an ideal pipe without fixed original magnetization, B_y-φ curve is exactly the same as that calculated by Eq. (5). Compared to the pipe with no original magnetization, the B_y-φ curves of pipes with different magnetizations are parallel with different offsets. The offset is caused by the fixed original magnetization. It indicates that the fixed original magnetization will introduce magnetic bias in a certain fixed direction inside the pipe. This magnetic bias will vary with the change of the size and number of fixed original magnetization of the pipe and must be removed.

According to Eqs. (6) and (7), λ_r is calculated by using the data in Fig. 6, and the results are shown in Fig. 6. Removing the magnetic DC bias is equivalent to removing the original magnetization of the pipe. With the bias removed, λ_r of the pipes containing different original magnetizations are identical. The calculated λ_r is independent of the angle between the pipe axis and the ambient field. It is proved that no matter what the original magnetization value is and whether the magnetization distribution is uniform or random, the influences of original magnetizations can be completely eliminated via DC-removing,

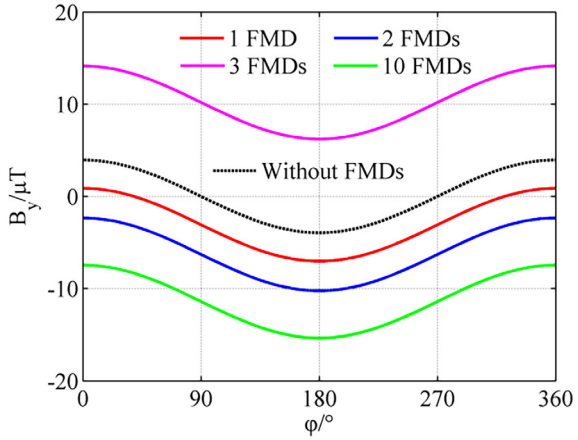

Fig. 5. B_y-φ curves of pipes containing different original magnetizations.

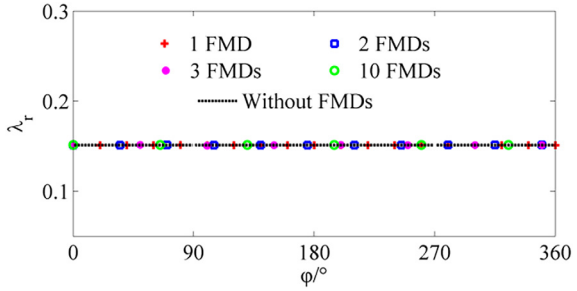

Fig. 6. Radial magnetic shielding factors of pipes calculated after removing DC biases.

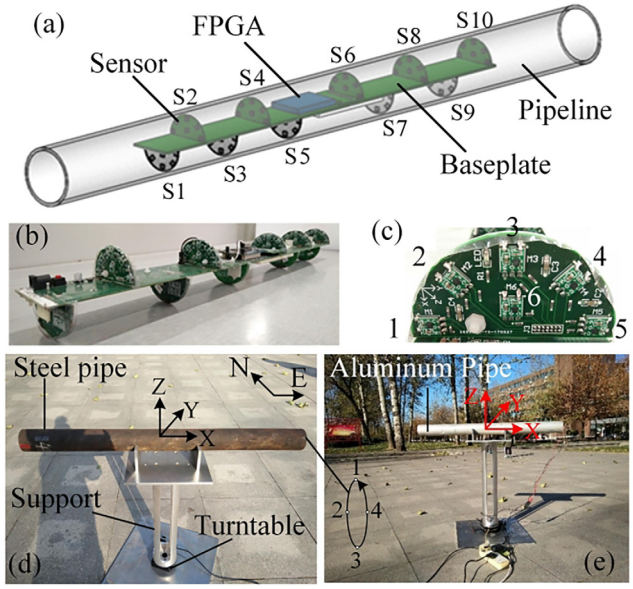

Fig. 7. Experimental method and apparatus.

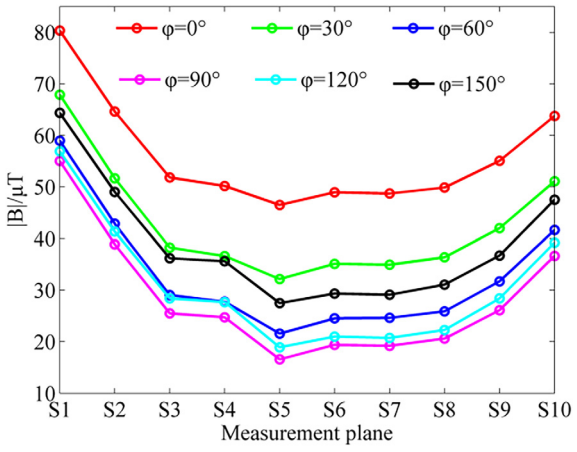

Fig. 8. Measured magnetic fields inside one steel pipe.

and the radial magnetic shielding factor can be exactly obtained. The magnetic permeability of the pipeline can be also exactly measured according to Eq. (3).

4. Experiments

Considering nonuniform distributions of the magnetic fields inside the pipe specimen, magneto resistive sensor array is used to measure the spacial magnetic fields, and a relatively uniform part in the middle

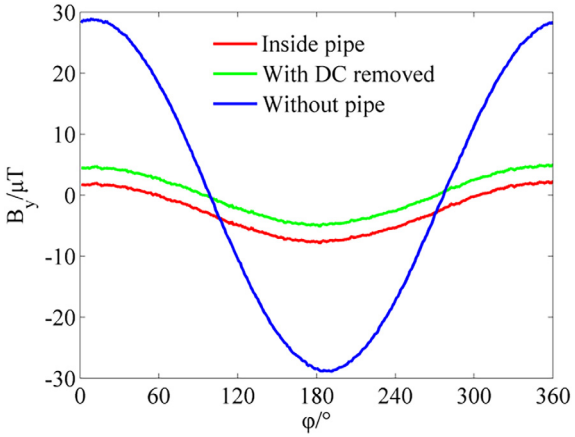

Fig. 9. Magnetic fields inside pipes and ambient fields at different rotation angles.

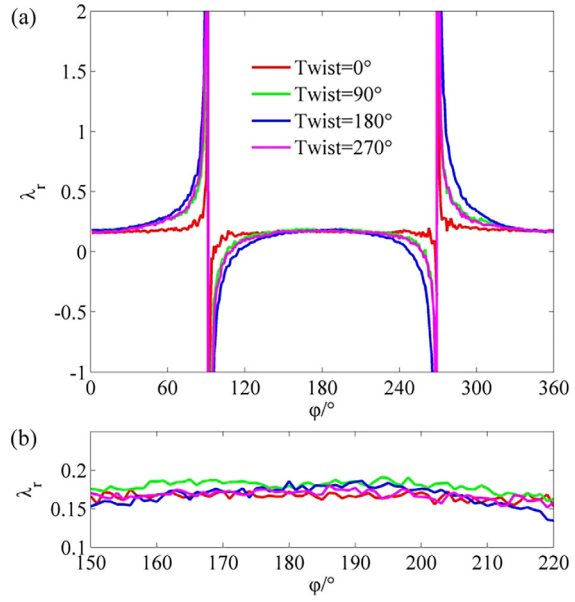

Fig. 10. Measured shielding factors of one steel pipe vs rotation angles.

Table 1
Measured permeabilities of pipes with different specifications.

Pipe number	Dimension Parameters/ mm			Shielding factor	Calculated permeability	
	D	*L*	*t*	λ_r	μ_r by Eq. (3)	μ_r by FEM
Pipe1,2#	80	500	4	0.1374	134.1689	135.5063
				0.1467	124.4554	125.6935
Pipe3–8#	80	1000	4	0.1712	103.9183	103.7714
				0.1582	114.0234	113.8628
				0.1800	97.9064	97.7668
				0.1666	107.3137	107.1635
				0.1326	139.7153	139.5203
				0.1279	145.5496	145.3487
Pipe9#	80	1500	4	0.1389	132.5142	131.9691
Pipe10#	80	2000	4	0.1716	103.6317	103.1413
Pipe11#	89	1	8.5	0.0700	155.7978	155.5332
Pipe12#	89	1.5	8.5	0.0775	139.7939	139.0792

is selected to calculate the shielding factor and permeability. As shown in Fig. 7(a), the magnetic field measurement system is placed inside the pipe. The sensors are evenly distributed on 10 measurement planes named S1–S10. Fig. 7(b) is a photograph of the assembled circuit board

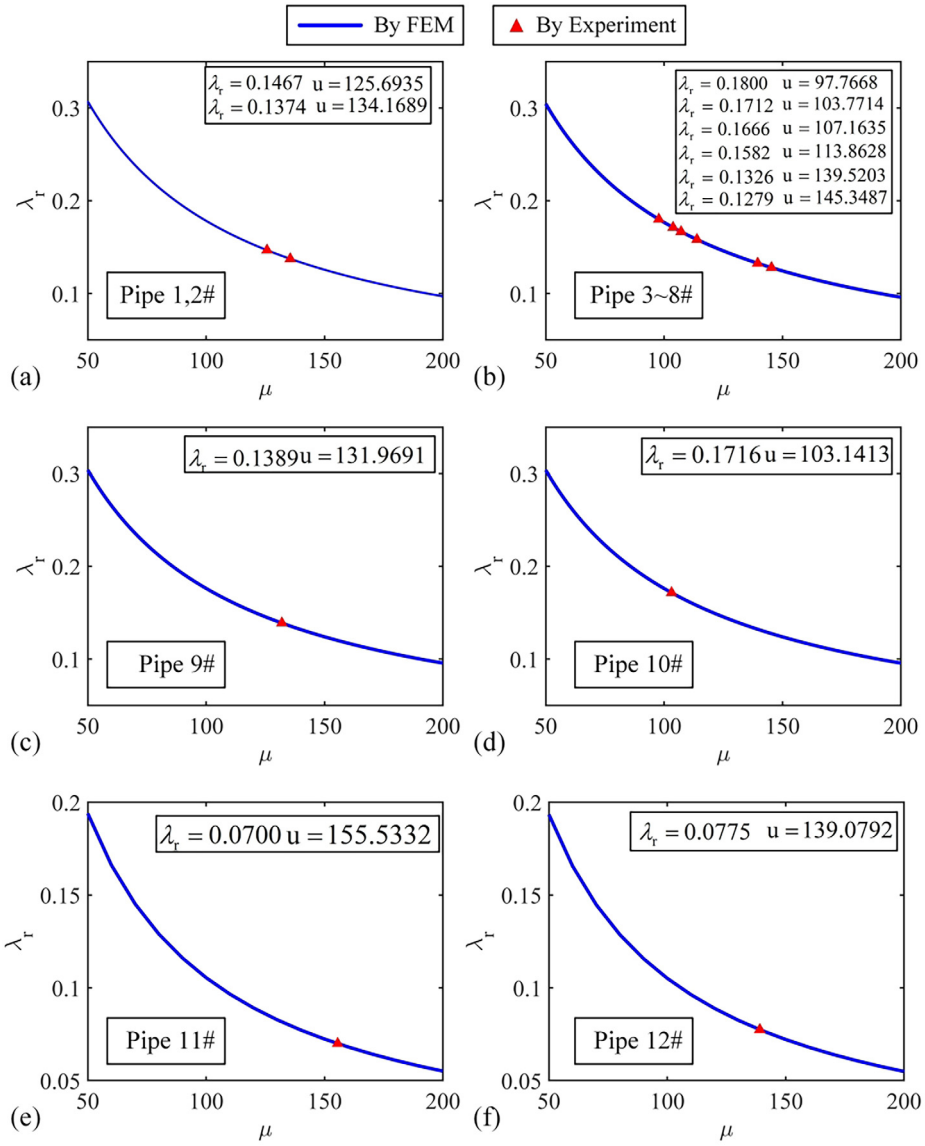

Fig. 11. Measured shielding factors and permeabilities perfectly overlap the simulation results of sweeping the permeability.

for magnetic measurements. As shown in Fig. 7(c), six magnetic sensors are evenly distributed on each semicircular measurement curve and one of them is located at the center. The data of each magnetic sensor are synchronously collected by the FPGA controller and uploaded to the computer through the USB bus for data analyses and magnetic permeability calculations.

The test site is selected in an open area to avoid any interference from other magnetic sources. As shown in Fig. 7(d), the computer controls the turntable carrying a steel pipe to rotate with a constant speed, and simultaneously measures and records the radial magnetic field component B_{mY}. There is a tall enough aluminum support between the steel pipe and the turntable motor, which keeps the steel pipe far away from the motor to avoid magnetic interference. For comparison as shown in Fig. 7(e), the ambient fields B'_{mY} in the same rotating frame are measured by using a non-magnetic aluminum pipe with the same size to hold the circuit board. Finally, the pipe permeability is calculated according to Eqs. (6), (7) and (3). A total of 12 different sizes of steel pipes are measured, with lengths of 0.5 m–2 m, wall thicknesses of 4 mm and 8.5 mm, and outer diameters of 80 mm and 89 mm. Each steel pipe is measured for four times. Each time the pipe is rotated by 90°around the X axis, namely, the twist angle takes four values of about 0°, 90°, 180°, 270° for each measurement.

The measured magnetic fields distributed along the axis inside one pipe rotating over six representative rotation angles are displayed in Fig. 8 as examples. It can be seen that as the rotation angle increases, the magnetic intensity inside the pipe decreases first and then increases, which corresponds to the increase and decrease of the included angle between the pipe axis and the ambient field. The magnetic fields inside are not uniform and noticeably vary near the pipe ends due to the edge effects. The magnetic fields in the middle of the pipe are flat and uniform, which is consistent with the measurement and analysis results in literature [23]. Therefore, measurement points on the middle planes S5-S7 will be used in the following experiments to reduce the measurement error of the shielding factor.

5. Results and discussions

The magnetic fields measured via rotating one steel pipe and one aluminum pipe on the turntable for one revolution are shown in Fig. 9, where the curves include B_y inside the steel pipe, B_y inside the steel pipe with DC removed, and B_y inside the non-magnetic aluminum pipe (ambient field). It can be seen that there is a large magnetic bias that needs to be removed in order to eliminate calculation error of the shielding factor. Fig. 10 shows the calculated radial shielding factor of

the pipe after the magnetic bias is removed. It can be seen that the radial shielding factor has two peaks at about $\varphi = 90^{\circ}$ and 270°. At these two rotation positions, the horizontal radial components of the magnetic fields inside and outside the pipe are both close to zero, so 0/0 occurs resulting in large singular values when calculating the shielding factor. At the remaining position, the measured shielding factor is mainly flat and smooth. It demonstrates that the magnetic shielding factor of the pipeline is independent of the rotation angle, except for the situation that the geomagnetic field is perpendicular to the pipeline axis. The average value of the flat section is taken as the final measured radial shielding factor of the pipe.

In order to improve the measurement precision, each steel pipe is measured for four times, and each time the pipe is rotated 90°around the radial axis, namely, the twist angle takes four values of about 0°, 90°, 180°, 270° for each measurement, as shown in Fig. 10(a). The middle flat section is zoomed in for each case, as shown in Fig. 10(b). The final measured shielding factor of each pipe is the average of the four measurements above. The four twist positions of the pipe are shown in Fig. 7.

The radial magnetic shielding factors of the pipes with different specifications were measured and the permeability of the pipes was calculated according to Eq. (3). The results are listed in Table 1. It can be seen that the shielding factors are dispersive in regards to different pipes. Even for pipes with the same size, the shielding factors are still different, which indicates that the relative permeabilities of the pipes are different. Permeability sweeping simulations of these pipes are carried out, and the curves of the radial shielding factor vs the permeability are obtained. Then the permeability values corresponding to the measured radial shielding factors are determined through linear interpolation on these curves. The results are listed in Table 1. The marked points in Fig. 11 are measurement values of the magnetic shielding factors and permeabilities. Although the measurement results are discrete for pipe with different sizes, there is always one permeability value on the simulation curve to make the measured shielding factor equal to the simulated one. Taking the later as a reference, the relative error of the proposed method is less than 1%. This demonstrates that it is accurate and efficient of the radial shielding factor formula based on the IPM to calculate the pipe permeability.

6. Conclusions

This paper demonstrates a method of measuring the permeability of a pipe immersed in the geomagnetic field based on the magnetic shielding effect. One pipe section, instead of a strip, rod, or ring cut from the pipe, is used as the testing specimen. During the measurement, the pipe is placed in an open area and rotates around the vertical axis. Magnetic fields inside the pipe are measured and the middle flat part are used to calculate the radial magnetic shielding factor and then the permeability. Finite element simulations and experiments demonstrate that:

(1) The IPM can accurately formulate the relationship among the radial shielding factor, wall thickness, diameter, length, and permeability of a pipe.
(2) Fixed original magnetizations of a steel pipe can induce magnetic bias inside the pipe. The bias can be accurately calculated and then removed by using the magnetic fields measured while the pipe is rotating. The magnetic fields with bias removed can be used to accurately calculate the shielding factor and the permeability of the pipe.
(3) As the tested short pipe is cut from a long one that has already gone through all the manufacture procedures, its permeability measured by this method is also that of a field pipeline and are therefore of great significance for the magnetic abnormal inspection of on-site pipelines.

Acknowledgments

This work is supported by National Natural Science Foundation of China (No. 61773283, 51604192, and 61473205) and Project funded by China Postdoctoral Science Foundation (No. 2018M630271).

References

[1] Liu Bin, He Luyao, Ma. Zeyu, Zhang Hai, Sfarra Stefano, Fernandes Henrique, Perilli Stefano, Study on internal stress damage detection in long-distance oil and gas pipelines via weak magnetic method, ISA Trans. 89 (2019) 272–280.
[2] Huang Xinjing, Chen Guanren, Yu. Zhang, Xu. Li Jian, Chen Shili Tianshu, Inversion of magnetic fields inside pipelines: modeling, validations, and applications, Struct. Health Monit. Int. J. 17 (1) (2018) 80–90.
[3] T.J. Sumner, J.M. Pendlebury, K.F. Smith, Convectional magnetic shielding, J. Phys. D Appl. Phys. 20 (9) (1987) 1095–1101.
[4] A. Mager, Magnetic shielding efficiencies of cylindrical shells with axis parallel to the field, J. Appl. Phys. 39 (3) (1968) 1914.
[5] Lu. Hongmin, Menglin Xue, Fu. Junmei, Analysis of magneto static shielding effectiveness of the infinite cavity cylinder with magnetic material, J. Xidian Univ. 26 (1) (1999) 80–83.
[6] Xinjing Huang, Shili Chen, Shixu Guo, Xu. Tianshu, Qianli Ma, Shijiu Jin, Gregory S. Chirikjian, A 3D localization approach for subsea pipelines using a spherical detector, IEEE Sens. J. 17 (6) (2017) 1828–1836.
[7] Zhao Wei, Huang Xinjing, Chen Shili, Zeng Zhoumo, Jin Shijiu, A detection system for pipeline direction based on shielded geomagnetic field, Int. J. Press. Vessels Pip. 113 (2014) 10–14.
[8] A. Zakeri, Review of state-of-the-art: drag forces on submarine pipelines and piles caused by landslide or debris flow impact, J. Offshore Mech. Arctic Eng. 131 (1) (2009) 403–410.
[9] J. Cai, X. Jiang, G. Lodewijks, Residual ultimate strength of offshore metallic pipelines with structural damage – a literature review, Ships Offshore Struct. 12 (8) (2017) 1037–1055.
[10] D.C. Jiles, Theory of the magnetomechanical effect, J. Phys. D Appl. Phys. 28 (8) (1998) 1537–1546.
[11] G.G. Bush, Measurement Techniques for Permeability, Permittivity and EMI Shielding: A Review, IEEE International Symposium on Electromagnetic Compatibility, IEEE, 1994.
[12] R. Langman, Measurement of reversible permeability using solid (nonlaminated) specimens, Electr. Eng. Proc. Inst. 117 (9) (1970) 1887–1890.
[13] Ziqiang Cui, Weiyang Zhang, Huaxiang Wang, Magnetic permeability measurement method for particle materials, IEEE Int. Instrum. Measure. Technol. Conf. (12MTC) (2018) 1–6.
[14] H. Qing, L. Zhengkun, A novel apparatus for measuring permeability of weak magnetic materials, IEEE Trans. Instrum. Meas. 54 (2) (2005) 730–733.
[15] J.M. Makar, B.K. Tanner, The in situ measurement of the effect of plastic deformation on the magnetic properties of steel Part II – permeability curves, J. Magn. Magn. Mater. 187 (3) (1998) 353–365.
[16] J.M. Makar, B.K. Tanner, The effect of stresses approaching and exceeding the yield point on the magnetic properties of high strength pearlitic steels, NDT&E Int. 31 (2) (1998) 117–127.
[17] R. Langman, A. Belle, D. Bulte, et al., Measuring the permeability of stressed steel by the magnetomotive-force-vane method with magnetization perpendicular to the surface, IEEE Trans. Magn. 39 (5) (2003) 2179–2189.
[18] Y. Yu, Y. Zou, M. Jiang, et al., Investigation on Conductivity Invariance in Eddy Current NDT and its Application on Magnetic Permeability Measurement, Ndt New Technology & Application Forum, IEEE, 2016.
[19] M. Lu, W. Zhu, L. Yin, et al., Reducing the lift-off effect on permeability measurement for magnetic plates from multifrequency induction data, IEEE Trans. Instrum. Meas. 99 (2017) 1–8.
[20] Zandong Han, Xiaoyang Li, Measurement of magnetic permeability and magnetic loss of structural steel for dynamic magnetization, J. Tsinghua Univ. 54 (11) (2014) 1471–1485.
[21] D. Desjardins, T.W. Krause, L. Clapham, Transient eddy current method for the characterization of magnetic permeability and conductivity, NDT&E Int. 80 (2016) 65–70.
[22] Luo Qingwang, Shi Yibing, Wang Zhigang, Zhang Wei, Ma. Dong, Research on the inversion of physical parameters of the ferromagnetic pipe, Chinese J. Sci. Instrum. 37 (1) (2016) 10–14.
[23] Huang Xinjing, Chen Shili, Guo Shixu, Zhao Wei, Jin Shijiu, Magnetic charge and magnetic field distributions in ferromagnetic pipe, Appl. Comput. Electr. Soc. J. 28 (8) (2013) 737–746.